Nanometer-Sized Gold Particles Supported on SiO_2 by Deposition of Gold Sols from $Au(PPh_3)_3Cl$

G. Martra,*,† L. Prati,‡ C. Manfredotti,† S. Biella,‡ M. Rossi,‡ and S. Coluccia†

Dipartimento di Chimica I.F.M., Università di Torino, via P. Giuria 7, I-10125 Torino, Italy, and Dipartimento di Chimica I.M.A, Università di Milano, via Venezian 21, I-20133 Milano, Italy

Received: December 3, 2002; In Final Form: March 11, 2003

An Au/SiO_2 system with most of the metal particles less than 2.0 nm in size were prepared by deposition on silica of preformed gold sols derived from $Au(PPh_3)_3Cl$. In this form, it was inactive in the $CO + O_2$ reaction at ca. 333 K, because of the presence of phosphine ligands on the surface of metal particles. The system became catalytically active in this reaction after treatment in O_2 at 673 K, which also resulted in a slight sintering of the metal phase (mean size = 2.9 nm). By subsequent heating in H_2 at 673 K, the mean size of gold particles increased up to 3.4 nm. Such particles exhibited a lower amount of step surface sites able to adsorb CO, but became more active in the $CO + O_2$ reaction. This suggested that the reaction steps involving oxygen can occur more effectively on Au sites present on larger and smoother gold particles.

1. Introduction

Since the finding by Haruta et al.[1] of unique catalytic performances in low-temperature CO oxidation of nanosized gold particles, several preparation methods have been investigated and optimized for the dispersion of Au at a nanometric level, resulting in heterogeneous catalysts which are highly effective in that reaction and also in a number of other oxidation processes in the gas phase, such as complete oxidation of hydrocarbons,[2a] oxygenated hydrocarbons,[2b] and amines,[2c] hydrogenation of carbon oxides,[3] unsaturated hydrocarbons,[4] and carbonyl compounds,[5] the water shift reaction,[6] reduction of nitrogen oxides,[7] and halogen compound decomposition.[8] As reviewed by Haruta,[9] the three preparation methods which appear most widely used are coprecipitation, deposition−precipitation, and chemical vapor deposition. More recently, Iwasawa and co-workers developed a new method based on the use of Au phosphine complexes as precursors of metal particles and freshly precipitated wet metal hydroxides as precursors for oxide supports.[10] Moreover, the preparation of supported gold catalysts for low-temperature CO oxidation via "size-controlled" gold colloids has been reported also.[11] The immobilization of preformed gold sols, both on oxides and on carbon, was used by us as a promising procedure for obtaining catalysts highly effective also in selective oxidation in the liquid phase.[12] In these studies, gold sols were prepared in the presence of different types of protecting agents, and it was recently demonstrated that the original particle size in the sol is maintained after immobilization only if the protecting agent and the support are chosen accurately.[12c] However, the stability of the dispersion of such supported gold particles and the evolution of their properties upon the removal of the protecting agent and thermal treatments in different atmospheres have not been investigated yet. In this paper, we consider a system prepared by immobilization on silica of a preformed gold sol obtained by reduction of mononuclear gold complex $Au(PPh_3)_3Cl$ and then treated in O_2 and H_2 atmosphere. Silica is usually considered ineffective as a support for the dispersion of gold in a catalytically active form, mainly because of the difficulty of depositing it on such an oxide by traditional methods. Coprecipitation and conventional deposition−precipitation fail in the preparation of Au/SiO_2 catalysts, mainly because the point zero charge (PZC) of silica is around pH 2, and then at pH 7 this oxide exhibits a large negative surface charge, which does not allow the deposition of $Au(OH)_3$. Impregnation with either $HAuCl_4$[13] or cationic Au−phosphine cluster[14] solutions produced very large supported Au particles (mean size ≥ 16 nm), after calcination, catalytically inactive for CO oxidation at room temperature. However, the use of sol−gel methods for the deposition of gold on SiO_2, with the addition of amines as stabilizers of the metal phase, resulted in the formation of Au particles with an average size of 5−6 nm,[15] useful for catalytic purposes. Also chemical vapor deposition (CVD) was successfully applied in obtaining silica-supported gold particles small enough (mean size ca. 6.6 nm) to be active for CO oxidation, even at temperatures lower than 273 K.[13] This evidence indicates that, per se, also SiO_2 can be regarded as a useful support for catalytically active nanosized gold particles. Moreover, the attractiveness of silica materials as supports for gold catalysts increased following reports on Au particle growth within the channels of MCM-type mesoporous silicas.[16] Au nanoparticles on SiO_2 are actively investigated also in the field of glasses doped with metal and semiconductor nanoparticles, because their nonlinear optical behavior may imply applications as photonic materials.[17−19]

Our study was focused on the evolution of the dispersion of supported gold particles depending on the removal of the stabilizing ligands and of the atmosphere in which thermal treatments were carried out, by checking, at each step of the treatment sequence, their activity in CO oxidation at room temperature (by IR, in model batch conditions) and their optical absorption features.

* Corresponding author: Voice: +39-011-6707538. Fax: +39-011-6707855. E-mail: gianmario.martra@unito.it.

† Università di Torino.

‡ Università di Milano.

10.1021/jp0225166 CCC: $25.00
Published on Web 05/17/2003

2. Experimental

2.1. Materials. Gold of 99.999% purity in sponge and PPh_3 of the highest purity grade from Fluka were used to prepare the $Au(PPh_3)_3Cl$ precursor according to the procedure described in the literature.[20] The reduction of Au(I) was performed adapting the method employed for the preparation of $[Au_9(PPh_3)_8(NO_3)_3]$.[21] $Au(PPh_3)_3Cl$ (0.128 mmol) was dissolved in ethanol (128 mL), and then, under vigorous stirring, a 0.3 N solution of $NaBH_4$ in EtOH:H_2O 2:1 v/v (2 mL) was added dropwise at room temperature. The clear solution turned dark brown and after few minutes 2.5 g of SiO_2 (BET_{SSA} = 419 m^2 g^{-1}, P.V. = 2 mL g^{-1}, from Grace) were added under stirring. After 10 h, the slurry was filtered and the powder was dried in air at 373 K for 4 h. The resulting metal loading was 1 wt %, as checked by ICP analysis of the filtrate. The dried sample will be hereafter referred to as the "as prepared" Au/SiO_2 catalyst. High-purity O_2, H_2, and CO (Matheson) were employed in the activation treatments and in the adsorption and reaction experiments without any further purification except liquid nitrogen trapping.

2.2. Methods. Diffuse reflectance (DR) UV−Vis−NIR measurements were performed by a Perkin-Elmer *Lambda-19* spectrophotometer equipped with an integrating sphere. $BaSO_4$ was used as a standard, and the reflectance data were converted in the Kubelka−Munk function $F(R_\infty)$. The samples, in the form of powder, were introduced in a reflectance cell with an optical quartz window.

Transmission IR spectra (4 cm^{-1} resolution) of self-supporting pellets (ca. 5 mg cm^{-2}) placed in a conventional quartz cell equipped with KBr windows were recorded at beam temperature (b.t., ca. 333 K) by a Bruker IFS113v spectrometer.

Cells used for DR UV−Vis−NIR and IR measurements were attached to conventional vacuum lines (residual pressure: 1×10^{-6} Torr; 1 Torr = 133.33 Pa), and allowed all thermal treatments, adsorption−desorption, and reaction experiments to be carried out in situ. Thermal treatments were as follows:

·*O_2 Treatment*. After outgassing at room temperature (r.t.) for 1 h, 100 Torr O_2 was admitted in the cell and the sample was heated at 473 K for 1 h and outgassed at the same temperature for 1 h. This kind of treatment was carried out also by heating and outgassing the sample at 573 and 673 K. The sample treated at the highest temperature will be hereafter referred to as $Au/SiO_2-(O_2)$.

·*H_2 Treatment*. The $Au/SiO_2-(O_2)$ sample was put in contact at r.t. with 100 Torr H_2, heated at 673 K for 1 h and outgassed at the same temperature for 1 h. Such a treated sample will be hereafter referred to as $Au/SiO_2-(O_2/H_2)$.

The treatment procedure employed allowed the complete removal of H_2O molecules produced during reduction; accordingly, no additional bands resulting from adsorbed water were observed in the spectrum of these treated samples, which appeared identical to that of the $Au/SiO_2-(O_2)$ sample (spectra not reported).

For the transmission electron microscopy (TEM) investigations, carried out with a JEOL 2000EX instrument, a small amount of the samples used for the DR UV−Vis−NIR measurements was extracted from the cell and ultrasonically dispersed in isopropyl alcohol. A drop of the suspension was deposited on a copper grid covered with a lacey carbon film. Histograms of the particle size distribution were obtained by considering at least 300 particles on the TEM images, and the mean particle diameter (d_m) was calculated as $d_m = \Sigma d_i n_i / \Sigma n_i$, where n_i was the number of particles of diameter d_i.

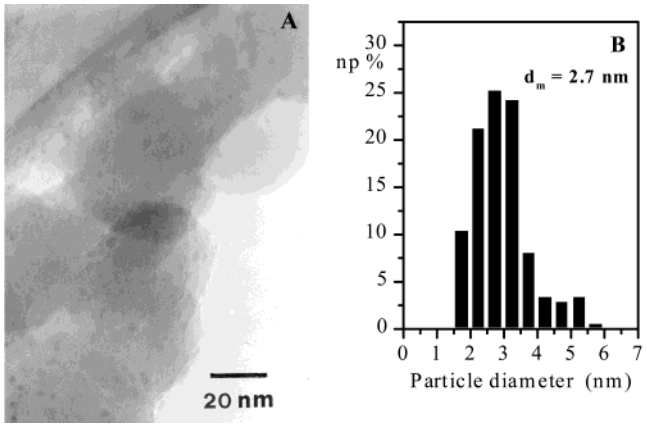

Figure 1. (A) Electron micrograph of the as prepared Au/SiO_2 sample; original magnification: 200000×. (B) Histogram of the metal particle size distribution.

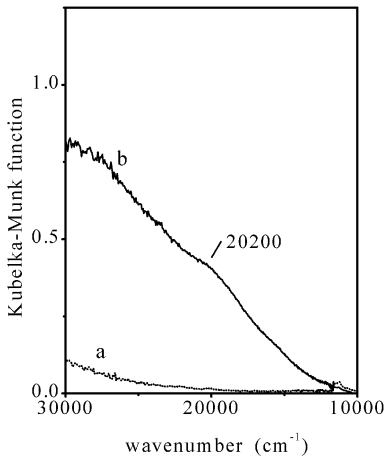

Figure 2. Diffuse reflectance UV−Vis−NIR spectra of (a) the bare SiO_2 support and (b) the as prepared Au/SiO_2 sample.

3. Results and Discussion

3.1. Study of the Dispersion of the Metal Phase by TEM and DR UV−Vis−NIR Spectroscopy. *3.1.1. The As Prepared Catalyst*. In Figure 1A, a TEM image representative of the as prepared catalyst is reported, where a few small metal particles, widely distributed on the support, are visible. The statistical analysis of their dimension (see Experimental) gave a metal particle size distribution (MPSD) in the 1.0−6.0 nm range (Figure 1B) and a mean diameter d_m = 2.7 nm.

As a complementary source of information on the dispersion of the metal phase, DR UV−Vis−NIR analysis was performed. In the case of the bare support, only a very weak absorption at frequencies higher than 20000 cm^{-1} was observed, likely a result of metal ions present at an impurity level (Figure 2, a), whereas the spectrum of the as prepared Au/SiO_2 sample exhibited a continuous absorption with the onset at ca. 10000 cm^{-1} and increasing in intensity as the wavenumber increases, with a poorly defined local maximum at 20200 cm^{-1} (Figure 2, b).

Nanosized metals exhibit a surface-plasmon absorption in the visible region due to the collective oscillation of the conduction electrons in response to optical excitation, the position and width of this absorption depending on the particle size.[22,23] Detailed studies on the optical properties of gold nanocrystals with very narrow size distribution evidenced that such a structureless absorption is characteristic of Au particles less than 2.0 nm in size, while larger particles were found to produce a defined plasmonic peak.[24,25] On this basis, the optical spectrum obtained

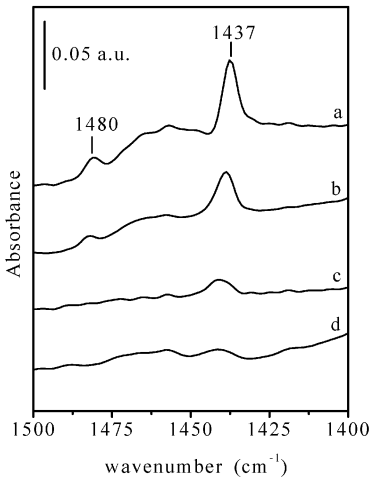

Figure 3. FTIR spectra of the Au/SiO_2 catalyst; curve (a) spectrum of the as prepared sample, after outgassing at beam temperature for 1 h; curves b−d: after treatment in O_2 (100 Torr) for 1 h and at (b) 473, (c) 573, and (d) 673 K, and subsequent outgassing 1 h at the same temperatures.

for the as prepared Au/SiO_2 sample (Figure 2, b) suggests that it should mainly contain gold particles smaller than 2.0 nm. By contrast, particles less than 2.0 nm in size appeared to represent only ca. 10% of those observed in TEM images (Figure 1B). This discrepancy can be rationalized by considering that TEM measurements suffer a lack of sensitivity for very small metal particles that usually escape the detection by this technique when they are less than 1.0 nm in size. Furthermore, even larger but very thin supported metal particles might be hardly observable, owing to their poor contrast. It can be then proposed that the as prepared sample mainly contains Au particles less than 2.0 nm in size, as suggested by DR UV−Vis−NIR data, but most of them are too small or thin to be revealed by TEM. Gold particles with size in the 2.0−6.0 nm range, clearly observed in the electron micrographs, might contribute to the weak band partially emerging at 20200 cm^{-1}.

3.1.2. Effect of Removal of Phosphine Ligands by Heating in O_2. The IR spectrum in the 1500−1400 cm^{-1} range of the as prepared Au/SiO_2 sample outgassed at beam temperature exhibits a sharp peak at 1437 cm^{-1} and a weaker component at 1480 cm^{-1} (Figure 3, a), associated with semicircular stretching modes of the aromatic rings of the triphenylphosphine ligands.[26] Other bands characteristic of this compound, at frequencies higher than 3000 cm^{-1} (ν_{CH}) and lower than 1000 cm^{-1} (ν_{P-C}), were obscured by intense bands resulting from the ν_{OH} adsorption of hydrogen-bonded silanols and to the lattice modes of the support, respectively.

The phosphine bands progressively decrease in intensity by treating the sample in O_2 at increasing temperature (Figure 3, b−c) and disappear after treatment at 673 K (Figure 3, d), indicating that ligands are progressively oxidized and removed, in agreement with recent data on similar systems.[27]

The treatment in oxygen was accompanied by significant changes in the optical features of the sample (Figure 4), which turned from pale brown to violet. Instead of the structureless, broad plasmonic absorption observed in the case of the as prepared system (Figure 4, a), a well-defined plasmonic peak at 20000 cm^{-1} was present in the DR UV−Vis−NIR spectrum of the sample treated in O_2 at 673 K [$Au/SiO_2-(O_2)$ sample, Figure 4, b]. The narrowing of the plasmonic absorption can be ascribed to an increase of the size of gold particles,[18] suggesting that a sintering process of the metal phase occurred.

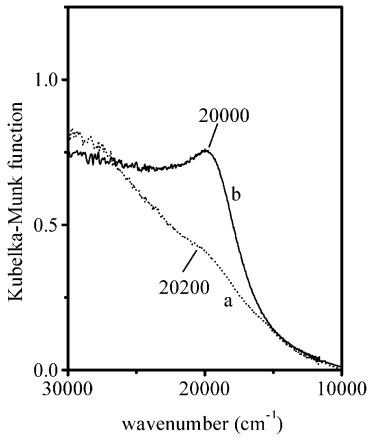

Figure 4. Diffuse reflectance UV−Vis−NIR spectra of (a) the as prepared Au/SiO_2 sample (the same as in Figure 2, b), and (b) the $Au/SiO_2-(O_2)$ sample.

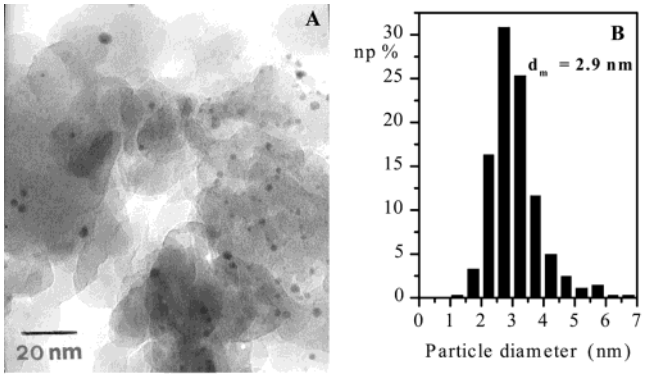

Figure 5. (A) Electron micrograph of the $Au/SiO_2-(O_2)$ sample; original magnification: 200000×. (B) Histogram of the metal particle size distribution.

TEM images of the $Au/SiO_2-(O_2)$ sample show a denser population of metal particles (Figure 5A), though their resulting size distribution was similar to that obtained for the as prepared one, except for a slight broadening toward larger diameters (Figure 5B). This suggests that the sintering process mainly involved gold particles which in the as prepared catalyst were too small and/or thin to be observed by TEM, resulting in an increase of the number of particles clearly detectable by this technique.

No significant changes either in the MPSD or in the optical spectrum were observed by further heating in oxygen at 673 K.

3.1.3. Effect of the Treatment in H_2. A subsequent treatment in H_2 at 673 K [$Au/SiO_2-(O_2/H_2$ sample)] modified the size distribution of the particles detectable by TEM, decreasing the fraction of particles smaller than 2.5 nm to 10% of the observed population and shifting the mean diameter to 3.4 nm (Figure 6). Accordingly, the plasmonic band slightly shifted to lower frequencies (maximum at 19900 cm^{-1}, spectrum not shown). However, the extent of the sintering appeared limited, and the width of the size distribution did not increase significantly. Heating in H_2 for a longer time did not result in further sintering of the metal phase.

3.2. FTIR Spectra of Adsorbed CO: Surface Features of Gold Particles. Figure 7 shows the IR spectra of CO adsorbed on the catalyst in the as prepared (part A), $Au/SiO_2-(O_2)$ (part B), and $Au/SiO_2-(O_2/H_2)$ (part C) forms. In all cases the bands due to adsorbed carbon monoxide reached their maximum intensity in the presence of 10 Torr CO, indicating that the saturation of the metal surface was achieved in that condition.

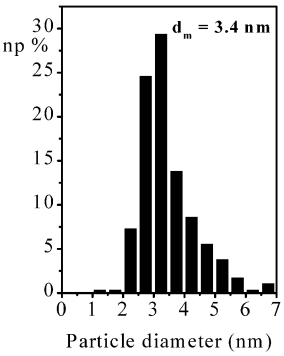

Figure 6. Histogram of the metal particle size distribution obtained by TEM analysis of the $Au/SiO_2-(O_2/H_2)$ sample.

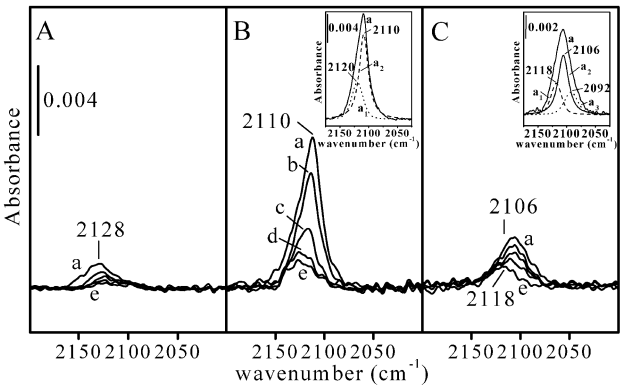

Figure 7. FTIR spectra of CO adsorbed under decreasing pressure on (A) the as prepared sample; (B) the $Au/SiO_2-(O_2)$ sample, and (C) the $Au/SiO_2-(O_2/H_2)$ sample. For all sections the different curves represents spectra taken in the presence of (a) 10, (b) 5, (c) 2, (d) 0.5 Torr CO and (e) after outgassing at beam temperature for 30 min. The full lettering in (A) and (C) is as in (B). Inset in (B): (a) experimental spectrum of CO (10 Torr) adsorbed on the $Au/SiO_2-(O_2)$ sample; (b, c) Lorentzian components resulting from the fit of curve (a). Inset in (C): (a) experimental spectrum of CO (10 Torr) adsorbed on the $Au/SiO_2-(O_2/H_2)$ sample; (b−d) Lorentzian components resulting from the fit of curve (a).

3.2.1. CO on the As Prepared Sample. The adsorption of CO on the as prepared sample outgassed at beam temperature (b.t.; ca. 333 K) produced a very weak band at 2128 cm^{-1}, progressively decreasing in intensity by decreasing the CO pressure and finally disappearing by brief outgassing at b.t. (Figure 7A, a−e). This absorption is in a region where bands due to CO coadsorbed with oxygen on gold sites were observed.[28] In fact, the exposure of the as prepared catalyst to air can result in a chemisorption of oxygen, which resists outgassing at b.t. The very weak intensity of this band indicates that only a few gold sites are available to CO adsorption, likely as a result of the presence of the phosphine ligands on the surface of gold particles.

3.2.2. CO on the $Au/SiO_2-(O_2)$ Sample. A significantly more intense band appeared by adsorbing CO on the $Au/SiO_2-(O_2)$ sample, where the ligands have been removed (Figure 7B, a). This complex band shows a maximum at 2110 cm^{-1} and a shoulder at ca. 2120 cm^{-1}, and its profile is well fitted by superposition of two Lorentzian bands centered in these positions (Figure 7B, inset). By decreasing the CO equilibrium pressure, the component at 2110 cm^{-1} progressively decreased in intensity and shifted to 2116 cm^{-1} (Figure 7B, b−d), and finally disappeared upon outgassing at beam temperature (Figure 7B, e). At the same time, the absorption at 2120 cm^{-1} underwent a significant decrease in intensity, accompanied by a shift to 2126 cm^{-1}, but did not disappear (Figure 7B, b−e). For both components, the shifts exhibited in dependence on coverage are due to coupling effects of CO oscillators, progressively fading away as their number decreases.[29]

The band at 2110 cm^{-1} can be assigned to CO molecules adsorbed on low-coordinated Au^0 sites in defect position (i.e. edges, corners, kinks).[23] The weaker component at 2120 cm^{-1} is located at higher frequency and exhibited a lower reversibility with respect to the main absorption at 2110 cm^{-1}. Both features indicate that the 2120 cm^{-1} band might be a result of CO molecules adsorbed on $Au^{\delta+}$ sites, where a partial positive charge is induced by interaction with the oxygen atoms of the support, as reported in the case of gold particles dispersed on other oxides.[28b] Interestingly, even silica appears able to exert this influence on supported metal particles, as found for the Cu/SiO_2 systems.[30] Notice that nanocrystalline copper has been a useful reference for the assignment of bands due to CO adsorbed on gold particles, owing to the similarity in surface electronic structure of these two metals.[31,32]

3.2.3. CO Adsorbed on $Au/SiO_2-(O_2/H_2)$ Sample. CO adsorption on the $Au/SiO_2-(O_2/H_2)$ sample produces a band at 2106 cm^{-1} (Figure 7C, a), slightly broader and significantly less intense than that observed for the $Au/SiO_2-(O_2)$ system. The lower intensity of the bands due to adsorbed CO results from the sintering of the metal phase promoted by the treatment in H_2 evidenced by TEM. Such sintering, although limited, is expected to affect significantly the sites able to adsorb CO, as they are atoms in defect position, such as kinks, steps, and corners.

Through a fitting procedure it was found that this band results from the overlapping of three Lorentzian components, located at 2118, 2106, and 2092 cm^{-1} (Figure 7C, inset). The absorptions at lower frequencies faded away by decreasing the CO coverage, while that at 2118 cm^{-1} was still observed after outgassing CO at b.t. (Figure 7C, b−e). The components at 2118 and 2106 cm^{-1} are close, though at slightly lower frequencies, to those observed for the $Au/SiO_2-(O_2)$ sample, and this suggests the same assignment to CO molecules adsorbed on $Au^{\delta+}$ and Au^0 sites in defect positions, respectively.

Because of its location at lower frequency, the minor component at 2092 cm^{-1} might be due to CO molecules stabilized on gold centers with a higher density of electronic charge. In the case of gold particles supported on n-semiconductor oxides, such sites were supposed to result from Schottky junction effects occurring at the contact perimeter of metal particles with the support.[33] Recently, it has been proposed that, for Au/TiO_2 and Au/ZrO_2 systems, F-centers formed at the surface of the support under reductive conditions can act as electron-donating centers toward metal particles.[34] Both these effects appear unlikely for Au nanocrystals dispersed on silica, an insulating oxide on which F-centers are not expected to be produced under the reductive treatment conditions adopted in this work. It can be tentatively proposed that such electron-rich surface metal centers in the $Au/SiO_2-(O_2/H_2)$ sample result from a reduction of some of the $Au^{\delta+}$ sites that were present after the oxidation treatments, sites rendered partially electropositive by the interaction with the oxygen atoms of the support. The suppression of this interaction decreases the contact area between the support and the gold particles and, therefore, between metal and oxide, further reducing any polarization effect on Au sites.

3.3. Performance in the CO + O_2 Reaction. *3.3.1. The As Prepared Sample.* As reported above, the admission of CO on the as prepared catalyst simply outgassed at beam temperature

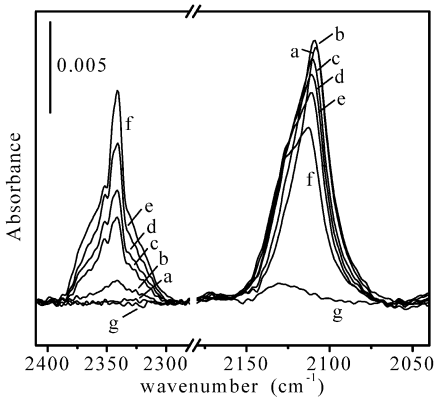

Figure 8. FTIR spectra of CO adsorbed on $Au/SiO_2-(O_2)$, treated in 100 Torr O_2 at 673 K for 1 h and outgassed at 673 K for 1 h, during reaction with O_2. Curve (a) is the spectrum in the presence of 10 Torr CO alone, curves (b−f): spectra recorded after admission of 10 Torr O_2 on preadsorbed CO: (b) immediately after O_2 inlet and after (c) 3.5, (d) 7.5, (e) 14.5, (f) 50 min of contact. Curve (g): spectrum recorded after outgassing of reaction mixture at beam temperature for 30 min.

produced a very weak band at 2128 cm^{-1}, as a result of CO adsorbed on a small fraction of accessible Au sites. The subsequent admission of O_2 in the cell did not produce any change in the spectral feature of adsorbed CO and no signal due to CO_2 was observed, even after 1 h of contact (spectra not reported), indicating that no reaction occurred. To obtain insight on the origin of the lack of reactivity, in a subsequent experiment O_2 was admitted first in the cell and then CO was added. No band due to CO_2 either to adsorbed CO was observed, indicating that the presence of oxygen prevented CO adsorption on Au sites. This result suggests that only isolated sites able to adsorb either CO or O_2 competitively are accessible on the surface of Au particles in the as prepared sample, the presence of the phosphine ligands preventing the exposure of sites where CO and O_2 can be coadsorbed.

3.3.2. The Au/SiO₂−(O₂) Sample. In the case of the $Au/SiO_2-(O_2)$ sample, the spectrum of preadsorbed CO (Figure 8, a) was significantly affected by the admission of O_2: the peak at 2109 cm^{-1} progressively decreased in intensity and shifted to 2115 cm^{-1}, while a new component grew up on its high frequency side, finally appearing as an evident shoulder at 2126 cm^{-1}. Significantly, a new band appeared at 2341 cm^{-1} (Figure 8, b−f) assignable to carbon dioxide molecules weakly interacting with the hydroxyl groups of the silica support, the stretching mode of which, initially located at 3742 cm^{-1}, was shifted downward by ca. 50 cm^{-1} (spectra not reported for the sake of brevity). The appearance of this band clearly indicates that the oxidation of a part of CO by O_2 occurred. On the other hand, the two components at 2115 and 2126 cm^{-1} can be ascribed to CO molecules left unreacted on the surface of gold particles, perturbed by the presence of coadsorbed oxygen in an atomic and molecular form, respectively.[35] CO molecules adsorbed in this form appeared highly reversible, as both the 2115 and 2126 cm^{-1} components disappeared almost completely by outgassing at beam temperature (Figure 8, g). The band due to CO_2 molecules, weakly held on the support, was also depleted.

CO was then readmitted on the catalyst, and a band with a maximum at 2112 cm^{-1} and an evident shoulder at 2126 cm^{-1} was obtained (Figure 9A1, a). The band appeared less intense and broader toward the high-frequency side with respect to that observed for CO adsorbed on the freshly activated sample (Figure 9A1, b′). The high-frequency part of the spectrum of re-adsorbed CO corresponds to that of CO left adsorbed on gold

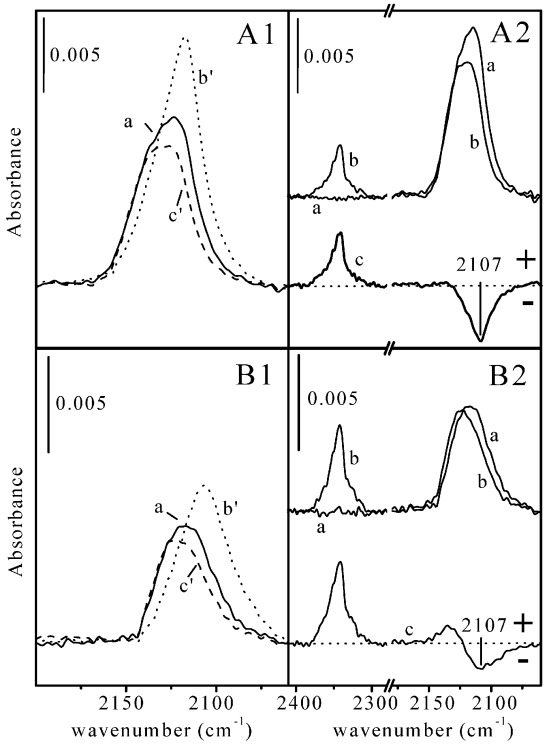

Figure 9. Section A: FTIR spectra of CO adsorbed on $Au/SiO_2-(O_2)$ treated in 100 Torr O_2 at 673 K for 1 h and outgassed at 673 K for 1 h, at different steps of the CO + O_2 reaction runs. Frame A1: (a) readmission of 10 Torr CO after the first reaction run and outgassing at beam temperature, (b′) 10 Torr of CO on the freshly activated sample, and (c′) CO adsorbed on gold at the end of the first reaction run. Frame A2: (a) spectrum of re-adsorbed CO (10 Torr) before the admission of O_2 (the same as curve (a) in section A1) and (b) spectra recorded at the end of the second CO + O_2 reaction run; (c) difference spectrum between (a) and (b). Section B: FTIR spectra of CO adsorbed on $Au/SiO_2-(O_2/H_2)$ at different steps of the CO + O_2 reaction runs. Frame B1: (a) readmission of 10 Torr CO after the first reaction run and outgassing at beam temperature, (b′) 10 Torr of CO on the freshly activated sample and (c′) CO adsorbed on gold at the end of the first reaction run. Frame B2: (a) spectrum of re-adsorbed CO (10 Torr) before the admission of O_2 (the same as curve (a) in section B1) and (b) spectra recorded at the end of the second CO + O_2 reaction run; (c) difference spectrum between (a) and (b).

particles at the end of the first reaction run (Figure 9A1, c′). This feature indicates that after the first CO + O_2 reaction run, inactive oxygen species were left on the surface of gold particles, resulting in the production of positivised $Au^{\delta+}$ sites in their neighborhood. On the other hand, only a small fraction of the Au^0 sites initially present on the fresh catalyst, which adsorb CO molecules responsible for the components at $\tilde{\nu} < 2115$ cm^{-1} of the spectrum in Figure 9A1, curve b′, was restored.

A subsequent admission of O_2 produced the depletion of the portion at $\tilde{\nu} < 2115$ cm^{-1} of the band due to adsorbed CO, while a band at 2341 cm^{-1} appeared again, indicating the formation of CO_2 (Figure 9A2). The part of the band depleted by interaction with O_2 was better evidenced by subtracting the spectrum of CO adsorbed before the contact with O_2 (Figure 9A2, a) from that recorded after the accomplishment of the reaction (Figure 9A2, b). The result, reported in Figure 9A2, c, exhibits a broad negative band, centered at 2107 cm^{-1} corresponding to CO initially adsorbed on the metal surface and then consumed during the reaction, while the positive peak at 2341 cm^{-1} evidences the production of CO_2.

No increase of the absorption due to CO adsorbed on $Au^{\delta+}$ sites was observed, indicating that all the Au centers which

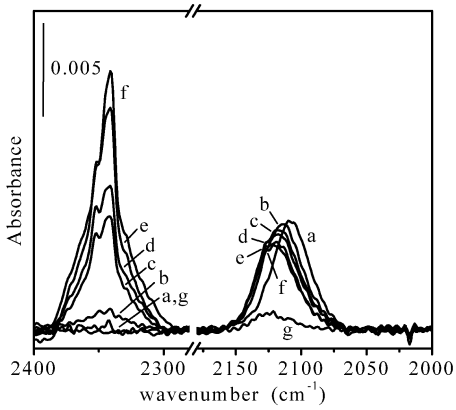

Figure 10. FTIR spectra of CO adsorbed on $Au/SiO_2-(O_2/H_2)$ during reaction with O_2. Curve (a) spectrum in the presence of 10 Torr CO alone, curves (b−f): spectra recorded after admission of 10 Torr O_2 on preadsorbed CO: (b) immediately after O_2 inlet and after (c) 3, (d) 6, (e) 12.5, (f) 50 min of contact. Curve (g): spectrum recorded after outgassing of reaction mixture at beam temperature for 30 min.

adsorb CO and O_2 in an inactive form were already saturated by oxygen species in the previous CO + O_2 run.

After the accomplishment of the reaction, the cell was outgassed and CO and O_2 were admitted on the sample in the order again. The same spectroscopic evidences depicted in Figure 9A2 were obtained, indicating that the Au^0 sites left unchanged after the first CO + O_2 reaction experiment actually behave as stable active centers for the oxidation of CO.

3.3.3. The $Au/SiO_2-(O_2/H_2)$ Sample. The same series of CO + O_2 reactions were performed on the $Au/SiO_2-(O_2/H_2)$ sample.

Immediately after the admission of O_2 on preadsorbed CO (Figure 10, a), the depletion of the low-frequency side of the band and a decrease in intensity of the band at 2106 cm^{-1} were observed, while a weak absorption at 2341 cm^{-1} due to CO_2 molecules appeared (Figure 10, b). By increasing the time of contact with O_2, the 2106 cm^{-1} band was progressively eroded, a new broader component grew up at 2120 cm^{-1}, and the absorption at 2341 cm^{-1} further increased in intensity (Figure 10, c−f). A subsequent outgassing of the cell resulted in the disappearance of this last band, and in a strong decrease in intensity of that at 2120 cm^{-1} (Figure 10, g). The overall behavior of the $Au/SiO_2-(O_2/H_2)$ sample in the CO + O_2 reaction appeared then quite similar to that of the $Au/SiO_2-(O_2)$ one.

As in the case of the $Au/SiO_2-(O_2)$ sample, a readsorption of CO and a second CO + O_2 reaction run were carried out. The data obtained are reported in frames B1 and B2 of Figure 9, for the sake of comparison with the spectra obtained for the $Au/SiO_2-(O_2)$ sample, reported in the upper part of that figure. In the spectrum of CO readmitted on the sample after the first CO + O_2 reaction run (Figure 9B1, a), the band of adsorbed CO appeared much weaker in intensity and shifted to higher frequency with respect to that observed before the first CO + O_2 reaction run (Figure 9B1, b′), but very similar to the spectrum obtained at the end of the reaction (Figure 9B1, c′), only exhibiting a slightly higher intensity on the high-frequency side. Noticeably, the component at 2092 cm^{-1}, specific to CO adsorbed on the freshly activated $Au/SiO_2-(O_2/H_2)$ sample (see inset in Figure 7C), was completely absent.

A second run of the reaction of CO oxidation was then carried out, by admitting O_2 onto the re-adsorbed CO. In Figure 9B2, the comparison of the spectra recorded before (curve a) and after the reaction (curve b) is reported. It can be noticed that the contact with oxygen resulted in the erosion of a very small fraction of the low-frequency side of the band at 2120 cm^{-1}, accompanied by the appearance of the CO_2 band at 2341 cm^{-1} (Figure 9B2, b). As in the case of the $Au/SiO_2-(O_2)$ sample, the component of the absorption at 2120 cm^{-1} depleted during the reaction was more clearly identified in the difference spectrum (Figure 9B2, c) obtained by subtracting the spectrum of CO adsorbed before the contact with O_2 (Figure 9B2, a) from that recorded after the accomplishment of the reaction (Figure 9B2, b).

It appears as a broad and featureless negative signal, still spread on the 2125−2050 cm^{-1}, with a poorly defined maximum at ca. 2107 cm^{-1}. The very weak intensity of the negative band indicates that only a very small fraction of Au^0 sites able to promote the reaction between CO and O_2 are left after the first run of CO oxidation.

3.3.4. Comparison between the Activity of the $Au/SiO_2-(O_2)$ and $Au/SiO_2-(O_2/H_2)$ Samples. Though quantitative conclusions require proper catalytic tests, qualitative indications on the activity of the $Au/SiO_2-(O_2)$ and $Au/SiO_2-(O_2/H_2)$ samples can be derived from the data described above, as the same mass of catalyst and the same experimental conditions were employed in the two cases. Furthermore, it has to be recalled that both samples were outgassed at 673 K prior to the IR measurements, and no water molecules likely produced during the treatment in H_2 were observed to be left adsorbed (see Experimental Section). This is an important point, because the presence of water can significantly affect the behavior of supported gold catalyst in the CO + O_2 reaction.[36]

The comparison between the IR spectra of $Au/SiO_2-(O_2)$ and $Au/SiO_2-(O_2/H_2)$ in the presence of CO alone (Figure 8, a and Figure 10, a, respectively) and after the accomplishment of a first reaction run with O_2 (Figure 8, f and Figure 10, f, respectively) evidences that a lower amount of CO is initially adsorbed on the $Au/SiO_2-(O_2/H_2)$ sample, but a larger amount of CO_2 (monitored by the intensity of the IR band at 2341 cm^{-1}) is formed after reaction with O_2, indicating that this system contains surface sites with a higher activity in the CO oxidation. However, as shown above, in the first run the production of CO_2 results from the occurrence of the reaction on both the sites that are inactivated after the run and those that exhibit an actual catalytic behavior. Insights on the difference in activity of this second type of sites for the $Au/SiO_2-(O_2)$ and $Au/SiO_2-(O_2/H_2)$ systems were obtained by comparing their spectra taken at the beginning and at the end of the second reaction run (when only the "actual catalytic sites" are supposed to be able to convert CO), as well as the corresponding difference spectra (Figure 9A2 and B2). It can be noticed that the band resulting from the CO_2 produced by the reaction appeared slightly more intense in the case of the $Au/SiO_2-(O_2/H_2)$ sample (compare curves b in Figure 9A2 and 9B2), although the "apparent" amount of adsorbed CO consumed during the reaction, as monitored by the integrated intensity of the negative band centered at 2107 cm^{-1} (compare curves c in Figure 9A2 and B2) seemed to be lower. This features can be rationalized taking into account that CO molecules which undergo oxidation turn on the catalytic sites during the intervals between the recording of IR spectra, while these latter only monitored the amount of CO adsorbed on the sites in definite moments of the reaction. Thus, as the reaction time considered was the same for both the $Au/SiO_2-(O_2)$ and $Au/SiO_2-(O_2/H_2)$ samples, the fact that a higher amount of CO_2 was obtained with the $Au/SiO_2-(O_2/H_2)$ catalyst, which conversely contained a lower number of catalytic sites for the conversion of CO, indicates that on this

catalyst CO oxidation occurred with a higher turnover frequency. However, this difference with respect to the $Au/SiO_2-(O_2)$ sample cannot result from a difference in the type of active sites adsorbing CO, as the position of the component due to adsorbed CO (CO_{ads}) which is consumed during the reaction appeared similar in both cases. It can be then proposed that the higher yield of the $Au/SiO_2-(O_2/H_2)$ sample in the CO oxidation resulted from a difference in the efficiency of surface processes involving oxygen. For Au catalysts supported on hardly reducible oxides, such as SiO_2 and Al_2O_3, several studies suggested that the $CO + O_2$ reaction occurs on metal sites, without any role of the Au-oxide interface,[37,38] but the actual mechanism of oxygen adsorption and activation on gold sites is much in debate.

On one hand, it has been proposed that the CO oxidation starts with a $CO_{ads} + O_2 \rightarrow CO_2 + O_{ads}$ reaction (not belonging to a typical Langmuir−Hinshelwood mechanism), then is followed by a $CO_{ads} + O_{ads} \rightarrow CO_2$ reaction. On the other hand, it has been suggested that dissociation of O_2, producing adsorbed oxygen atoms O_{ads}, is the first step in the CO oxidation reaction, assumed in this case to belong to a Langmuir−Hinshelwood mechanism,[39,40] with a subsequent reaction between CO_{ads} and O_{ads}. This second step appears as a common feature for both types of proposed reaction pathways. The rate of this reaction should mainly depend on the strength of the adsorption of O_{ads} more than that of CO_{ads},[41] which decreases as the number of metal−metal bonds shared by the surface Au atoms acting as adsorbing sites for O atoms increases, according to the principle of bond energy−bond order conservation.[42]

Apparently, the surface structure of larger and smoother gold particles present in the $Au/SiO_2-(O_2/H_2)$ catalyst results in the presence of Au sites where the reaction of O_{ads} with CO_{ads}, can occur more effectively.

4. Conclusions

The deposition of preformed sols derived from $Au(PPh_3)_3Cl$ followed by a treatment in O_2 at 673 K has been found to be an effective method to obtain a highly dispersed Au/SiO_2 catalyst, with metal particle mean size of 3.0 nm, active in the $CO + O_2$ reaction at 333 K. This feature appears as a novelty for the preparation of gold catalyst supported on silica, as usually it was difficult to deposit on such oxide Au particles less than 5.0 nm in size.

Furthermore, the fact that a slight sintering and smoothing of metal particles by treatment in H_2 at 673 K resulted in a decrease of the amount of Au sites able to adsorb CO but in an increase of the activity in the $CO + O_2$ reaction suggests that on larger and smoother gold particles sites able to enhance the reactivity of adsorbed oxygen atoms are present.

Acknowledgment. Authors are grateful to Prof. Flora Boccuzzi for helpful discussion and to the Referees for stimulating comments. Financial support from MURST and INCA are acknowledged.

References and Notes

(1) Haruta, M.; Yamada, N.; Kobayashi, T.; Iijima, S. *J. Catal.* **1989**, *115*, 301.

(2) (a) Haruta, M.; Ueda, A.; Bamwenda, G. R.; Taniguchi, R.; Azuma, M. *Proceedings of the International Workshop on Catalytic Combustion*, Tokyo, April, 1994, pp 2−9; (b) Haruta, M.; Ueda, A.; Tsubota, A.; Torres Sanchez, R. M. *Catal. Today* **1996**, *29*, 443; (c) Ueda, A.; Haruta, M. *Shigen Kankyo Taisaku (Resources and Environment)* **1992**, *28*, 1035.

(3) (a) Sakurai, H.; Tsubota, S.; Haruta, M. *Appl. Catal. A: General* **1993**, *102*, 125; (b) Sakurai, H.; Haruta, M. *Appl. Catal. A: General* **1995**, *127*, 93.

(4) Ahn, H. G.; Sieun, Y.; Imamura, K.; Nakamura, R.; Niiyama, H. *Proc. 57th Annual Meeting Chem. Eng. Soc. Jpn.* **1992**, 300.

(5) Shibata, M.; Kawata, N.; Masumoto, T.; Kimura, H. *J. Chem. Soc., Chem. Commun.* **1988**, 154.

(6) Andreeva, D.; Idakiev, V.; Tabakova, T.; Andreev, A. *J. Catal.* **1996**, *158*, 354.

(7) (a) Qiu, S.; Onishi, R.; Ichikawa, M. *J. Phys. Chem.* **1994**, *98*, 2719.

(8) (a) Aida, T.; Higuchi, R.; Niiyama, H. *Chem. Lett.* **1990**, 2247; (b) Takita, Y.; Imamura, T.; Mizuhara, Y.; Abe, Y.; Ishihara, T. *Appl. Catal. B: Environmental* **1992**, *1*, 79.

(9) (a) Haruta, M. *Catal. Today* **1996**, *36*, 153; (b) Haruta, M. *Catal. Surveys Jpn.* **1997**, *1*, 61; (c) Haruta, M. *Stud. Surf. Sci. Catal.* **1997**, *110*, 123.

(10) . Kozlov, A. I.; Kozlova, A. P.; Liu, H; Iwasawa, Y. *Appl. Catal. A: General* **1999**, *182*, 9.

(11) Grunwaldt, J.-D.; Keiner, C.; Wögerbauer, C.; Baiker, A. *J. Catal.* **1999**, *181*, 223.

(12) (a) Prati, L.; Martra, G. *Gold Bull.* **1999**, *32*, 96; (b) Coluccia, S.; Martra, G.; Porta, F.; Prati, L.; Rossi, M. *Catal. Today* **2000**, *61*, 165; (c) Bianchi, C.; Porta, F.; Prati, L.; Rossi, M. *Top. Catal.* **2000**, *13*, 231; (d) Prati, L.; Rossi, M. *J. Catal.* **1998**, *176*, 552.

(13) Okumura, M.; Nakamura, S.; Nakamura, T.; Azamura, M.; Haruta, M. *Catal. Lett.* **1998**, *51*, 53.

(14) Yuan, Y.; Asakura, K.; Wan, H.; Tsai, K.; Iwasawa, Y. *Catal. Lett.* **1996**, *42*, 15.

(15) (a) Barathi, S.; Lev, O. *J. Chem. Soc., Chem. Commun.* **1997**, 2303; (b) Barathi, S.; Lev, O. *Anal. Commun.* **1998**, *35*, 29.

(16) Chen, C.; Zhang, Z.; Zhang, L. *Chem. Lett.* **2001**, *2*, 152.

(17) (a) Ricard, D.; Roussignol, Ph.; Flytzanis, Chr. *Opt. Lett.* **1985**, *10*, 511; (b) Hache, F.; Ricard, D.; Flytzanis, C.; Kreibig, K. *Appl. Phys.* **1988**, *A47*, 347.

(18) Dutton, T.; Van Wonterghem, B.; Saltiel, S.; Chestnoy, N. V.; Rentzepis, P. M.; Shen, T. P.; Rogovin, D. *J. Phys. Chem.* **1990**, *96*, 1100.

(19) . Matsuoka, J.; Mizutani, R.; Nasu, H.; Kamiya, K. *J. Ceram. Soc. Jpn.* **1992**, *100*, 599.

(20) Braunstein, P.; Lehner, H.; Matt, D. *Inorg. Synth.* **1990**, *27*, 218.

(21) Cariati, F.; Naldini, L. *J. Chem. Soc., Dalton Trans.* **1972**, 2286.

(22) Bohren, C. F.; Huffmann, D. R. *Absorption and Scattering of Light by Small Particles*; Wiley: New York, 1983.

(23) Kreibig, U.; Genzel, L. *Surf. Sci.* **1985**, *156*, 678, and references therein.

(24) Alvarez, M. M.; Khoury, J. T.; Schaaff, T. G.; Shafigullin, M. N.; Vezmar, I.; Whetten, R. L. *J. Phys. Chem.* **1997**, *101*, 3706.

(25) Link, S.; El-Sayed, M. A. *J. Phys. Chem. B* **1999**, *103*, 8410.

(26) Colthup, N. B.; Daly, L. H.; Wiberley, S. E. *Introduction to Infrared and Raman Spectroscopy*, 2nd ed.; Academic Press: New York, 1975; p 581.

(27) Kozlova, A. P.; Kozlov, A. I.; Sugiyama, S.; Matsui, Y.; Asakura, K.; Iwasawa Y. *J. Catal.* **1999**, *181*, 37.

(28) (a) Boccuzzi, F.; Chiorino, A.; Tsubota, S.; Haruta, M. *Catal. Lett.* **1994**, *29*, 225; (b) Boccuzzi, F.; Chiorino, A.; Tsubota, S.; Haruta, M. *J. Phys. Chem.* **1996**, *100*, 3625.

(29) Ruggiero, C.; Hollins, P. *Surf. Sci.* **1997**, *377*, 538.

(30) Boccuzzi, F.; Coluccia, S.; Martra, G.; Ravasio, N. *J. Catal.* **1999**, *184*, 316.

(31) Dumas, P.; Tobin, R. G.; Richards, P. L. *Surf. Sci.* **1986**, *171*, 555.

(32) Knell, A.; Barnickel, P.; Baiker, A.; Wokaun, A. *J. Catal.* **1992**, *137*, 306.

(33) Boccuzzi, F.; Tsubota, S.; Haruta, M. *J. Electron Spectrosc. Relat. Phenom.* **1993**, *64/65*, 241.

(34) Schimpf, A.; Lucas, M.; Mohr, C.; Rodemerck, U.; Brückner, A.; Radnik, J.; Hofmeister, H.; Claus, P. *Catal. Today* **2002**, *72*, 63.

(35) Boccuzzi, F.; Chiorino, A. *J. Phys. Chem. B* **2000**, *104*, 5414.

(36) Datè, M.; Haruta, M. *J. Catal.* **2001**, *201*, 221.

(37) Liu, Z.-P.; Hu, P.; Alavi, A. *J. Am. Chem.* Soc. **2002**, *124*, 14770, and references therein.

(38) Bond, G. C.; Thompson, B. T. *Gold. Bull.* **2000**, *33*, 41, and references therein.

(39) Heiz, U.; Sanchez, A.; Abbet, S.; Schneider, W.-D. *J. Am. Chem. Soc.* **1999**, *121*, 3214.

(40) Bollinger, M. A.; Vannice, M. A. *Appl. Catal. B: Environmental* **1996**, *8*, 417.

(41) Bondzie, V. A.; Parker, S. C.; Campbell, C. T. *Catal. Lett.* **1999**, *63*, 143.

(42) (a) Campbell, C. T. *Surf. Sci.* **1997**, *27*, 1; (b) Campbell, C. T. *Curr. Opin. Solid State Mater. Sci.* **1998**, *3*, 439.